Design of a double spring membrane for a two degree-of-freedom electromagnetic vibration energy harvester

Matthias Perez, Kevin Billon, Simon Chesné, Claire Jean-Mistral, Sandrine Bouvet, Christian Clerc

Design of a double spring membrane for a two degree-of-freedom electromagnetic vibration energy harvester

Matthias PEREZ[1], Kévin BILLON[1], Simon CHESNE[1], Claire JEAN-MISTRAL[1], Sandrine BOUVET [2] and Christian CLERC[2]

[1]Université de Lyon, CNRS INSA-Lyon, LaMCoS UMR5259, avenue Jean Capelle, F-69261, Villeurbanne, France
[2]Vibratec, 28 chemin du petit bois, F69130, Ecully, France

matthiasperez1@gmail.com

Abstract

This paper reports on the design of a cm-scale double spring membrane used in a two degree-of-freedom electromagnetic vibration energy harvester for railway monitoring applications. This type of membrane design enables to achieve very low stiffness for the springs (typically between 1N.mm^{-1} up to 10N.mm^{-1}) in one piece, which reduces manufacturing losses and greatly simplify the system assembly. In addition, they are very thin, resulting in extremely compact devices, which is very important in energy harvesting. The mechanical modelling of different types of membranes was performed using a finite element approach in order to highlight the best geometry. A series of membranes have been manufactured by machining into a non-magnetic steel and tested with the entire energy harvester.

1 Electromagnetic vibration energy harvester

Structural Health Monitoring (SHM) of railway structures [1-3] need autonomous and robust sensors leading to the development of electromagnetic energy harvester operating under harsh environment (choc, dust…). In order to characterize the vibratory environment of a tramway in operation, several accelerometers were placed on a Citadis 402 bogie. This enabled us to collect a significant number of data on the infrastructure of Lyon's tramway [4-5] used as an input parameter and implemented in a multi-physic model. Figure 1 shows the power spectral density associated with all these measurements, it may thus be observed two predominant frequencies at f_1=33Hz and f_2=62Hz.

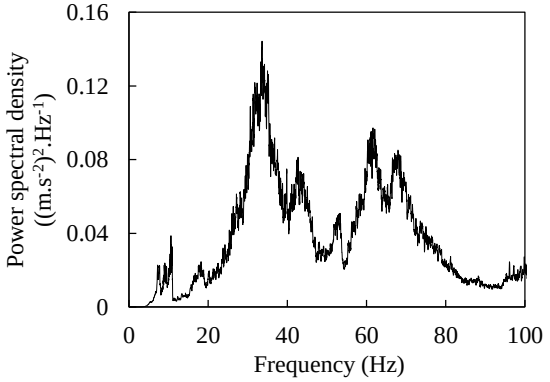

Figure 1: Power spectral density averaged over almost five hours of measurements on a Citadis® 402 bogie.

Under this specific excitation, we previously shown in [4-5] that it was interesting to use a two degree-of-freedom (DoF) vibration energy harvester instead a single DoF system. In this way, the two parts of the harvester can be tuned to resonate at two different frequencies, in order to be perfectly adapted to the spectrum of the input signal. As an electromagnetic converter is considered, the first DoF is composed of a stack of permanent magnets (in blue in Figure 2a) and the second DoF is made up several coils (in green in

Figure 2a). In order to obtain two resonators, a minimum of two linear springs must be added (in red in Figure 2a). Both are linked to a common frame (in black in Figure 2a) which is intended to be fixed on the tramway. Figure 2b and 2c show respectively the permanent magnet stack and the cylindrical coils.

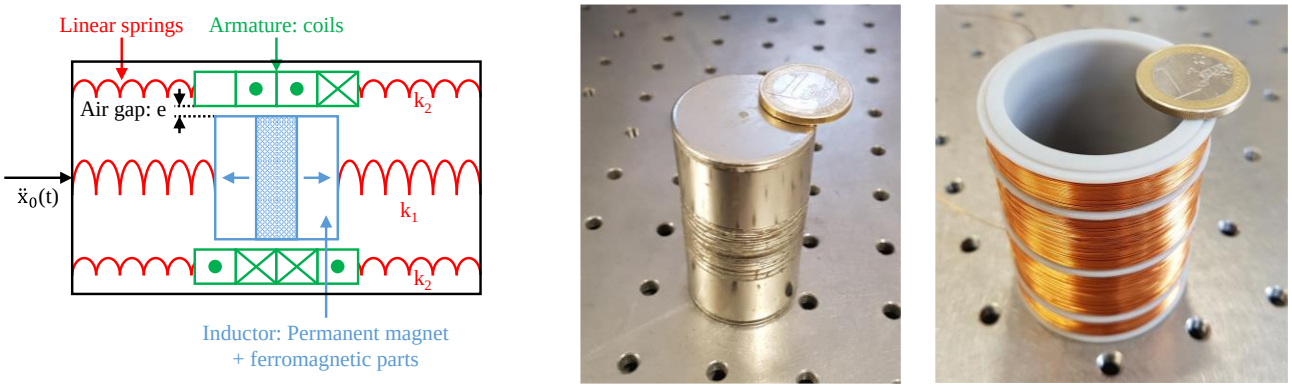

(a) (b) (c)

Figure 2: (a) Schematic representation of a 2 DoF inertial device. (b) Picture of a cylindrical permanent magnet stack. (b) Picture of an hollow cylinder coils.

2 Design of the spring membranes

Linear spring can be obtained with a lot of different shapes. For our electromagnetic energy harvester, the aim is to develop: (i) a light spring able to operate the range 10-100Hz, and also (ii) able to ensure high levels of acceleration with (iii) low embedded size and weight. Double membrane springs with a disk shape could be the solution for our design of a two DoF energy harvester. Let's first study a single membrane spring (k_1) and then extend our conclusions to a double membrane spring (k_1 and k_2).

2.1 Shapes studied and stiffness analysis

The four types of membranes shown in Figure 3 will be studied, starting with a simple full disk membrane (Figure 3a) on which matter is progressively removed (Figure 3b up to 3d). Considering the mass of the permanent magnet stack and the coils (100-500g) and the desired first resonance frequencies (26-27Hz), the stiffness targeted for membrane spring k_1 ranges between $k=1N.mm^{-1}$ and $10N.mm^{-1}$

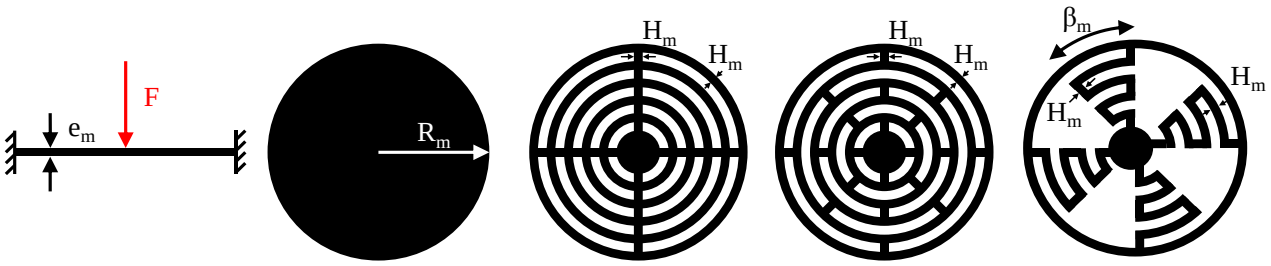

(a) (b) (c) (d)

Figure 3: Shape of the different membranes studied in this paper: (a) "disk" membrane, (b) "type 1" membrane, (c) "type 2" membrane, (d) "type 3" membrane.

Finite Element simulations using Ansys software have been done on each membrane described in Figure 3, in a clamped configuration with a punctual central force applied on it. From our finite elements computations, one can reviewed that the stiffness of the membrane spring is proportional to the Young modulus of the material (E), to the cube of the membrane thickness (e_m^3) and inversely proportional to the square of the radius (R_m^{-2}). This last point is valid provided that the thickness of the membrane is small compared to the radius of the membrane, i.e. $e_m << R_m$.

Thus, this implies that it is possible to set the stiffness of the membrane spring by changing the material properties (its Young modulus), the thickness of the membrane or the type of membrane (the radius of the membrane is set by the dimensions of the harvester). In what follows, a stainless steel disk membrane will be used as a reference (black curve in the FE simulations shown in Figure 4). For this type of membrane, it can be observed in Figure 4a that the membrane thickness should be drastically reduced in order to obtain low stiffnesses (typically between 1 and 10 $N.mm^{-1}$). For "type 1" and "type 2" membranes, it can be seen in Figure 4a and Figure 4b that the decrease of the thickness of the concentric bands (H_m) results in a significant reduction of the stiffness. Similarly, Figure 4c and Figure 4d indicate that "type 3" membranes can reach low stiffnesses by reducing the width of the bands (H_m) or by increasing the forming angle of each circular sector (β_m).

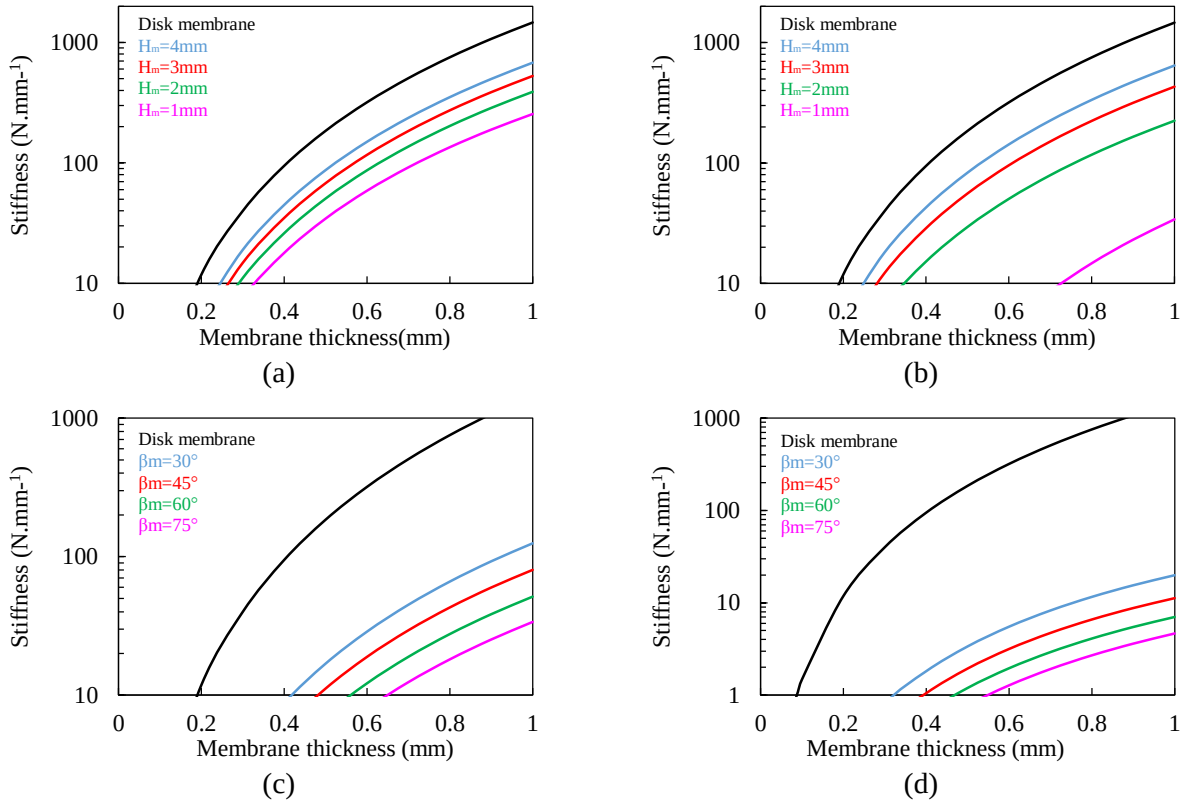

Figure 4: Examples of stiffnesses associated with: (a) "type 1" membranes, (b) "type 2" membranes. "Type 3" membranes with (c) H_m=2mm, and (d) H_m=1mm. All these data have been calculated using Ansys® with E=200GPa (stainless steel), a radius R_m=25mm and N_m=4 circular sectors.

2.2 Mechanical limits and strain analysis

For a particular design of a spring membrane, it is possible to check with our finite elements analysis that the maximum stress developed into the spring membrane is directly proportional to the force applied (F) and inversely proportional to the square of the thickness (e_m^2); for $e_m << R_m$ and within the limits of the elastic deformations of the membrane's material.

For a specified stiffness, the main idea is thus to identify the membrane which is able to withstand the highest force F and to develop the lowest stresses on the membrane (σ_{max}). Figure 5 shows the evolution of the ratio σ_{max} /F as a function of the stiffness for the different types of membranes previously mentioned. The main idea is thus to identify the membrane which enables to obtain a characteristic curve σ_{max} /F as low as possible. For stainless steel 304 for example, the yield strength is equal to σ_{max}=250MPa. Therefore, if we want to achieve a stainless steel 304 membrane with a radius R_m=25mm and a stiffness equal to $2N.mm^{-1}$, it is possible to consider the following options:

- A **"disk"** membrane of **110µm** thick able to withstand a central force of approximately **1.52N**.
- A **"type 1"** membrane (H_m=1mm) of **191µm** thick able to withstand a central force of approximately **1.11N**.
- A **"type 2"** membrane (H_m=1mm) of **306µm** thick able to withstand a central l force of approximately **2.63N**.

- A **"type 3"** membrane (H_m=1mm, β_m=75°) of **720µm** thick able to withstand a central force of approximately **3.57N**, which currently makes the "type 3" membrane the best option.

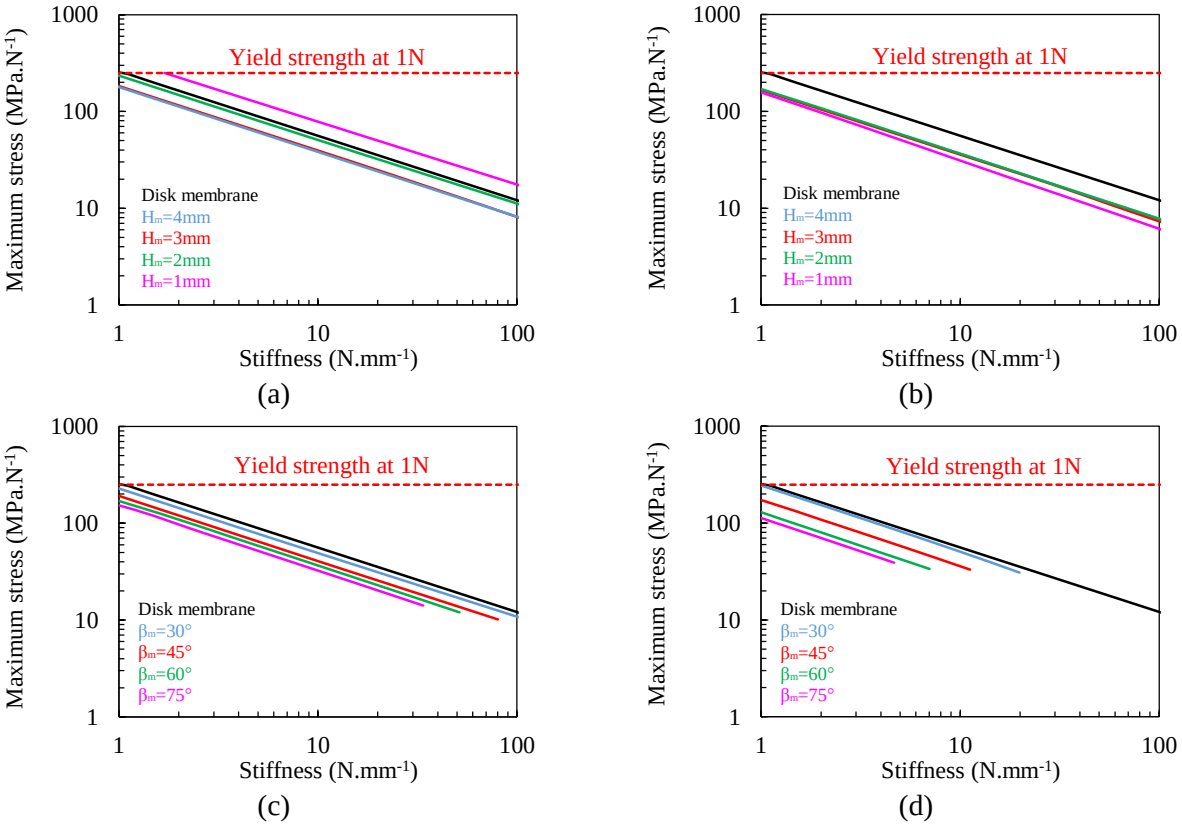

Figure 5: σ_{max} /F vs stiffness of the membrane: (a) "type 1" membranes, (b) "type 2" membranes. "Type 3" membranes with (c) H_m=2mm, and (d) H_m=1mm. All these data's have been calculated using Ansys® with E=200GPa (stainless steel), a radius R_m=25mm, and N_m=4 circular sectors.

Figure 6 illustrates the repartition of the stress on the surface of the membrane when a force is applied at its center. For "type 1" membranes, it can be noticed in Figure 6a that the mechanical stresses are concentrated on the external part of the membrane, which makes them very fragile. In Figure 6b, it can be observed that the mechanical stresses are better distributed over the "type 2" membrane, this design is then more robust as previously demonstrated. Finally, the "type 3" design does not significantly change the stresses distribution compared with the "type 2" design, as illustrated in Figure 6c. In contrast, the decrease of the stiffness associated with this specific design is such important that it is possible to apply substantial forces (Figure 6c and Figure 6d).

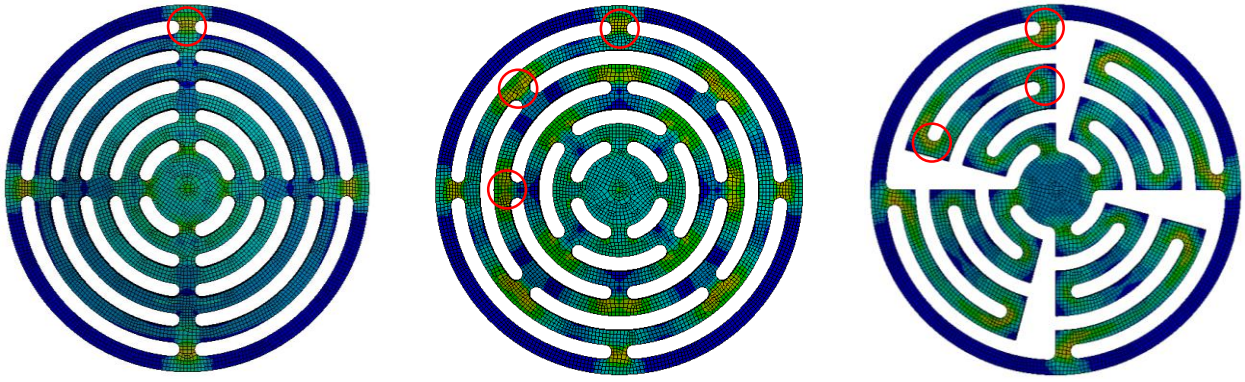

Figure 6: Visualization of the stresses distribution (von Mises) on three membranes: (a) "type 1",(b) "type 2", (c) "type 3", β_m=75°. In all three cases, R_m=25mm, H_m=3mm, and N_m=4 circular sectors.

3 Experimental results

3.1 Manufacturing of the membranes

As mentioned earlier, the energy harvester proposed in this paper is composed of a cylindrical permanent magnet stack (first DoF) surrounded by cylindrical coils (second DoF). In addition, as the stiffness associated with the first DoF is much lower than the stiffness associated with the second DoF, double spring membranes in stainless steel 304 presented in Figure 7a have been developed. The central part of the double spring membrane is composed of N_{m1}=3 circular sectors composed of 5 concentric bands of H_{m1}=1mm width, e_{m1}=800µm thickness and β_{m1}=100°. The lateral part of the double spring membrane is also composed of N_{m2}=3 circular sectors with the following parameters: H_{m2}=1mm, e_{m2}=800µm, β_{m2}=98°. This design provides a central stiffness of k_1=6.86N.mm^{-1} and a lateral stiffness equal to k_2=20.53N.mm^{-1} within the elastic range (Figure 7b). In Figure 7b, it can be highlighted that the yielding of the membrane theoretically occurs around 10N.

When assembling the device, the central ring (blue dotted line in Figure 7) is directly screw to the permanent magnet stack, the median ring (red dotted line in Figure 7) is glued to the outer casing while the outer ring (green dotted line in Figure 7) is fixed to the coils. This type of design provides two non-bulky membrane springs in a single piece, which could eventually lead to decrease manufacturing costs and greatly simplifies the final assembly.

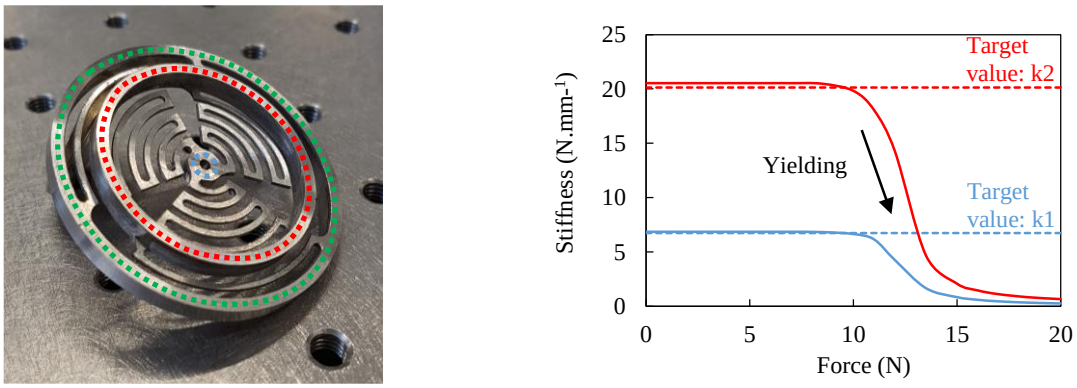

(a) (b)

Figure 7: Example of a double spring membrane in stainless steel 304. Central part: N_{m1}=3 circular sectors, e_{m1}=800µm, H_{m1}=1mm, β_{m1}=100°. Lateral part: N_{m2}=3 circular sectors, e_{m2}=800µm, H_{m2}=1mm, β_{m2}=98°. (a) Picture of the membrane, (b) Evolution of the two stiffnesses under different forces (EF simulations).

3.2 Application to a two degree-of-freedom electromagnetic inertial energy harvester

Two double spring membranes were assembled in a vibration energy harvester. These specific membranes have been designed and manufactured to provide resonance frequencies of the electromagnetic harvester about f_{01}=26Hz and f_{02}=63Hz, in order to maximize the energy extraction and conversion. Figure 8 shows the response of the energy harvester at different frequencies. We can thus observed a typical response of a two degree-of-freedom device, with f_{01} corresponding to the resonance frequency of the first DoF (permament magnet stack + central part of the double spring membrane) and f_{02} related to the resonance frequency of the second DoF (coils + lateral part of the double spring membrane).

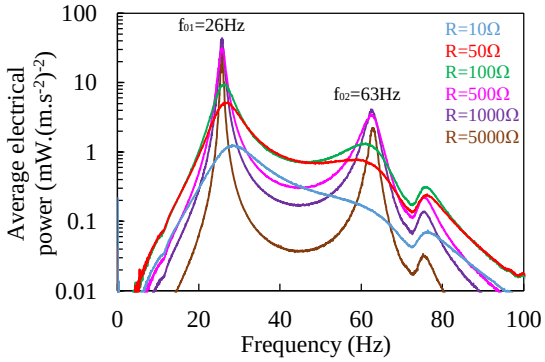

Figure 8: Typical transfer function of a two DoF prototype using double spring membranes.

This prototype has also been tested under real signals measured on a tramway and replicated on a test bench. For the optimal resistive load of 300 Ω, the average electrical power generated by the device is equal to 6.5mW, which means an average stored electrical energy of 700mJ by stations.

Conclusions

In this study, we reported on the numerical results obtained with four designs of membrane springs. The finite elements computations have allowed us to identify the most robust design ("type 3"), which was particularly helpful to develop and manufacture double spring membranes with very low stiffness (from 1 up to 10N.mm^{-1}). Some of these membranes were assembled in an electromagnetic vibration energy harvester intended to be placed on a bogie of a train or a tramway for the monitoring of railway structures. The average electrical power of the best prototype is equal to 6.5mW, which is equivalent to an electrical power density of 46.1mW.dm^{-3} and an electrical power mass density of 9.2mW.dm^{-3}.

Acknowledgement

The authors would like to thank the ADEME for the financial support of the MAVICO project on tramway monitoring, as well as Keolis for the test on Lyon tramway infrastructure.

References

[1] G. De Pasquale, A. Soma, and F. Fraccarollo, Piezoelectric energy harvesting for autonomous sensors network on safety-improved railway vehicles, Institution of mechanical engineers, part C: Journal of mechanical engineering science, 2011.

[2] J. Li, S. Jang, and J. Tang, Design of a bimorph piezoelectric energy harvester for railway monitoring, Journal of the Korean society for nondestructive testing, 2012.

[3] H. Park and J. Kim, Electromagnetic induction energy harvester for high-speed railroad applications, Precision engineering and manufacturing-green technology, 2016.

[4] M. Perez, S. Chesné, C. Jean-Mistral, K. Billon, S. Bouvet, and C. Clerc, A two degree-of-freedom electromagnetic vibration energy harvester for the railway infrastructure monitoring, Smart Materials, Adaptive Structures and Intelligent Systems, 2018.

[5] M. Perez, S. Chesné, C. Jean-Mistral, K. Billon, S. Bouvet, C. Clerc, Optimization of a two degree-of-freedom vibration energy harvester for a dual-frequency excitation, Recent Advances in Structural Dynamics, 2019.